



HAL
open science

Etched arrays of quantum well optical bistable microresonators

J. Oudar, T. Rivera, R. Kuszelewicz, F. Ladan

► **To cite this version:**

J. Oudar, T. Rivera, R. Kuszelewicz, F. Ladan. Etched arrays of quantum well optical bistable microresonators. *Journal de Physique III*, 1994, 4 (12), pp.2361-2370. 10.1051/jp3:1994282 . jpa-00249268

HAL Id: jpa-00249268

<https://hal.science/jpa-00249268>

Submitted on 4 Feb 2008

HAL is a multi-disciplinary open access archive for the deposit and dissemination of scientific research documents, whether they are published or not. The documents may come from teaching and research institutions in France or abroad, or from public or private research centers.

L'archive ouverte pluridisciplinaire **HAL**, est destinée au dépôt et à la diffusion de documents scientifiques de niveau recherche, publiés ou non, émanant des établissements d'enseignement et de recherche français ou étrangers, des laboratoires publics ou privés.

Classification

Physics Abstracts

42.65P — 78.47 — 81.40T

Etched arrays of quantum well optical bistable microresonators

J. L. Oudar ⁽¹⁾, T. Rivera ⁽¹⁾, R. Kuszelewicz ⁽¹⁾ and F. Ladan ⁽²⁾

⁽¹⁾ France TELECOM, CNET-Paris B, Laboratoire de Bagneux, B.P. 107, 92225 Bagneux Cedex, France

⁽²⁾ CNRS — Laboratoire de Microstructures et de Microélectronique, B.P. 107, 92225 Bagneux Cedex, France

(Received 9 February 1994, accepted 12 July 1994)

Abstract. — We report the operation of etched GaAs/AlGaAs multiple quantum well microresonators as low threshold all-optical bistable devices. The studied samples are 2-dimensional arrays of cylindrical microresonators of 6 μm height, with diameters of 4 μm and 6.4 μm . They are realized by SiCl_4 reactive ion etching of an epitaxial high finesse vertical microcavity structure. Due to the lateral carrier and light confinement, optical bistability is observed with a strongly reduced threshold power, below 100 μW for the 4 μm diameter devices. The optical confinement allows to achieve a high cavity Q factor in a reduced volume, and leads to the observation of multiple hysteresis loops due to the transverse mode structure of 6.4 μm diameter microresonators. The low bistability threshold, obtained without post-etching surface treatment, is attributed to a self-passivation occurring during the etching process, as evidenced by the observation of a thin coating film protecting the microresonator vertical surfaces.

The last decade has seen a growing interest in the combined use of micro-optics and semiconductor optoelectronic devices, in order to take advantage of the high interconnection capability of optics for information processing. This has been made possible by the progress in epitaxial techniques for the growth of semiconductor materials, which has resulted in the availability of high quality quantum wells embedded in high finesse single crystal vertical cavities, and in the development of micro-photonics devices, such as microlasers [1, 2] and nonlinear optical microcavities [3-6] with low operating powers and small vertical dimensions. In addition these structures are very interesting for the study of fundamental phenomena, such as microcavity effects, leading to strong modifications of spontaneous emission [7-9].

In this paper we discuss the properties of such nonlinear optical microcavities, used as all-optical bistable devices in a 2-dimensional array format. Such arrays make the best use of the specific geometry of vertical cavity devices, and allow to implement parallel architectures for optical information processing. In particular we describe the observation of all-optical bistability in etched vertical microresonators with transverse dimensions small enough to observe a significant reduction in bistability threshold power. This reduction, by more than a factor of 10, is due to the combined action of an efficient lateral confinement of light and

photoexcited carriers in a small multiple quantum well active volume. The paper is organized as follows. Section 1 describes the sample fabrication and its basic nonlinear optical and bistable properties. Section 2 discusses the light confinement provided by vertical waveguiding, and presents some experimental results on multiple hysteresis due to the switching between the transverse modes of these waveguides. Section 3 discusses the carrier confinement and a way to maintain the carrier lifetime in the ns range through self-deposition of a passivating film during the microresonator etching, and is followed by a conclusion.

1. Sample preparation and nonlinear optical properties.

In the present work we have combined two advances recently made in our laboratory : the realization of quantum well planar microcavities with much improved finesse and bistability threshold intensity [10], and the development of a two-step reactive Ion Etching (RIE) process providing smooth vertical surfaces and minimizing the density of surface recombination centers [11].

The vertical cavity structure, grown by organo-metallic vapor-phase epitaxy (OMVPE) on a GaAs substrate [12], consists of 23.5 periods of AlAs/Ga_{0.9}Al_{0.1}As quarter-wave thick layers acting as a bottom mirror, a 18.5-period MQW active medium consisting of 10 nm-thick Ga_{0.7}Al_{0.3}As barriers and 10 nm-thick GaAs wells, and 17 periods of the same AlAs/Ga_{0.9}Al_{0.1}As alternate layers acting as a front mirror. The theoretical finesse of this structure is in the range 500-800, depending on the absorption coefficient of the nonlinear medium. The maximum experimental finesse of this sample was 700 at a wavelength of 879 nm, corresponding to a Q -factor of $\sim 5\,000$. Due to the high cavity finesse, optical bistability with wide hysteresis loops was observed on this planar sample. The minimum bistability threshold intensity was measured to be as low as 350 W/m^2 (or equivalently $3.5\ \mu\text{W}/\mu\text{m}^2$) when measured with moderately focused incident beams ($30\ \mu\text{m}$ diameter). Upon tighter focusing, the threshold power could be decreased only to approximately 1 mW. Indeed in a non pixellated sample the threshold power does not scale simply with the spot area, because at small spot sizes diffusion laterally spreads the photoexcited carriers, and diffraction loss rapidly degrades the cavity finesse, as soon as the incident beam angular spectrum becomes wider than the angular width of the Fabry-Perot resonance [13].

In principle these problems can be solved by the carrier confinement and optical waveguiding provided by lateral sample structuring, i.e. pixellation. This is not an easy task however, because of the increased number of constraints that must be simultaneously fulfilled. One of the difficulties is that the carrier confinement is really useful only when the carrier lifetime is kept to a value close to that of the original unpixellated sample. Basically, two approaches have been pursued to achieve this lateral confinement : to remove the semiconductor material between the active devices, or to modify its composition to such an extent that it becomes inactive. The first approach makes use of dry etching techniques to make mesa-type microresonators. However up to now this has resulted in a drastic reduction of the carrier lifetime and of the magnitude of the nonlinear refractive index, through surface recombination [3-5]. The optical power necessary for nonlinear switching was much increased, so these microresonators could only be operated in the picosecond regime, but not in the quasi-steady-state required for optical bistability. The second approach makes use of alloy-mixing techniques to selectively transform the active multiple quantum wells into an inactive alloy between the individual devices [14, 15]. The advantages of this method are that the sample surface keeps its planarity, and that the carrier lifetime is preserved [16]. However the process involves a large number of technological steps, and requires the final deposition of a highly reflective dielectric mirror. In addition, the amount of lateral optical confinement is limited by the refractive index contrast between the quantum well and alloy regions (of the order of 0.01),

while the etching approach leads to a much larger refractive index difference. Our approach here has been to improve the etching technique in order to minimize the amount of surface recombination.

The technological process was performed as follows. A 1.5 μm thick Si_3N_4 layer was deposited by plasma-enhanced chemical vapor deposition (PECVD) on the sample surface. After standard photolithography and lift-off, a 100 nm aluminium mask was obtained. This mask was then transferred to the Si_3N_4 layer using CHF_3/SF_6 RIE. The Si_3N_4 layer was then used as a mask during the epitaxial structure etching, which was performed with SiCl_4 in a GIR 440 Alcatel RIE reactor, at a pressure of 8 m Torr and a power of 95 W. The etching speed was approximately 1 nm/s, corresponding to a total etching time of 90 mn for the whole structure. The 100 to 200 nm thick Si_3N_4 layer remaining after the etch would allow, in an extension of this work, a selective epitaxial regrowth of AlGaAs embedding the microresonators and planarizing the structure. The scanning electron micrograph displayed in figure 1 shows the good verticality of the devices, the presence of a remaining Si_3N_4 layer and the quality of the etched bottom surface.

The optical characteristics of these microresonators were measured with an amplitude-modulated laser beam generated by an Ar-pumped Ti-sapphire continuous-wave ring-cavity laser. The incident beam was circularly polarized in order to collect efficiently the colinearly reflected light, and it was focused to a diameter of 7 μm at half-intensity. Linear reflectivity spectra in a reference zone close to the etched microresonators indicated a finesse of 500 and a resonance wavelength of 869.05 nm, consistent with measurements performed on this sample prior to etching.

Optical bistability was studied by sending triangular pulses of 1 μs duration (full width at half-maximum) onto the microresonators and tuning the laser wavelength on the short

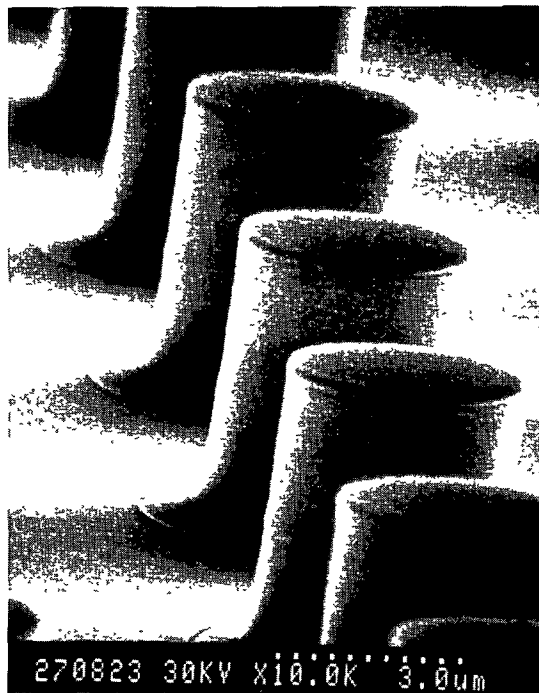


Fig. 1. — Scanning electron micrograph of 4 μm diameter microresonators.

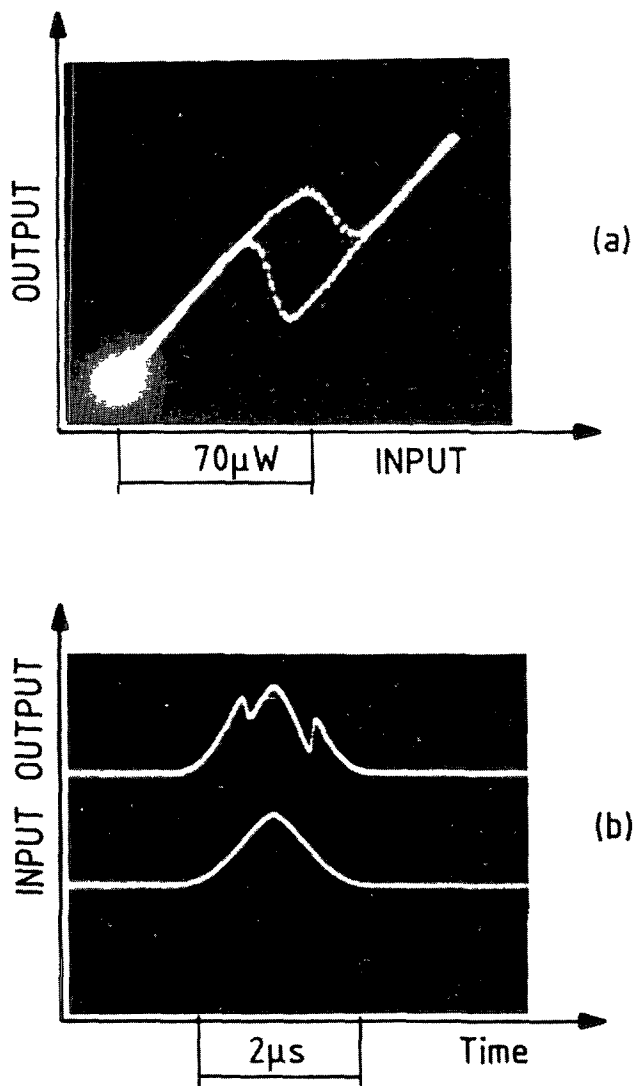


Fig. 2. — Bistable behaviour obtained on the $4\ \mu\text{m}$ microresonators. (a) Hysteresis observed with triangular-shaped input pulses; the incident power is calculated from equation (2). (b) Temporal evolution of the incident power (bottom trace) and the reflected power (top trace).

wavelength side of the Fabry-Perot resonance. Figure 2a shows the hysteresis loop obtained by displaying on a digital oscilloscope the reflected power vs. the incident power, obtained on microresonators of $4\ \mu\text{m}$ diameter, at a wavelength of $868.23\ \text{nm}$. The temporal evolution of the incident and reflected signals is displayed in figure 2b. A further evidence of the quasi steady-state bistable behaviour of these microresonators is displayed in figure 3, which shows that two stable reflectivity values are obtained for the same incident power below $100\ \mu\text{W}$, a lower reflectivity being observed after the short spike occurring at the center of the incident pulse.

The incident power P_{inc} intercepted by the microresonator is evaluated by integrating, over the circular microresonator aperture of radius r , the Gaussian intensity profile of the incident

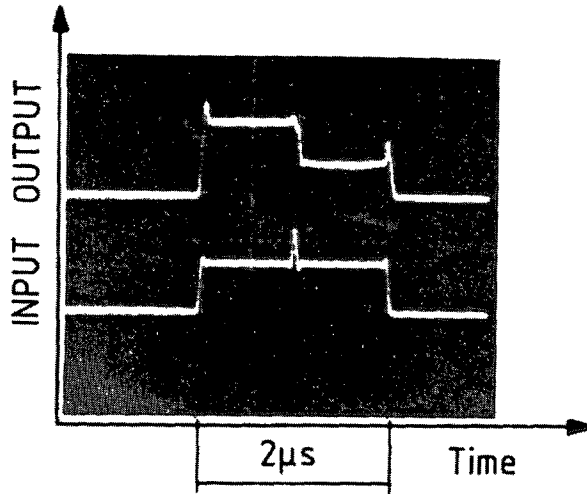


Fig. 3. — Direct evidence of steady-state bistability on the 4 μm microresonators. Bottom trace : incident power vs. time : top trace : reflected power vs. time.

beam of $1/e^2$ radius w . In this way P_{inc} is related to the total beam power P_{tot} through the relation

$$P_{\text{inc}} = P_{\text{tot}}[1 - \exp(-2r^2/w^2)]. \quad (1)$$

The relevant values for the result shown in figure 2a are $r = 2 \mu\text{m}$ and $w = 6 \mu\text{m}$, which gives a ratio $P_{\text{inc}}/P_{\text{tot}} = 0.20$. At the center of the hysteresis loop, the incident optical power intercepted by the microresonator was only $70 \mu\text{W}$, which is a significant threshold reduction compared with the 1 mW value obtained by tight focusing on this same sample prior to etching. We note that the corresponding power density is $5.6 \mu\text{W}/\mu\text{m}^2$, which is only slightly larger than the initial power density threshold of the planar sample. This indicates that the nonlinear refractive index and the cavity finesse are not degraded by the etching process, so that the size reduction of the active volume directly translates into a threshold power reduction, due to an efficient light and carrier confinement. These two aspects are discussed in the following.

2. Optical confinement.

Let us now emphasize the essential role of optical confinement in the present experimental results. Vertical waveguiding was necessary in order to maintain a cavity finesse as high as 500, in spite of the strong focusing of the incident beam. This can be understood as follows.

In a Fabry-Perot cavity with plane mirrors such as the present multilayer structure, it is well known that the resonant eigenmodes are plane waves, and that for propagation directions at an angle θ with respect to normal incidence their eigenfrequencies increase proportionately to $1/\cos \theta$. For an incident beam of finite lateral size such as a focused Gaussian beam, one may consider it as a superposition of plane waves with various in-plane wavevector components κ , so the overall cavity response can be expressed as the convolution product of the κ -dependent resonance lineshapes with this plane-wave distribution. When the Gaussian beam axis is normal to the plane of the cavity mirrors, the problem has a cylindrical symmetry, so that a Hankel transform may be used for the plane-wave decomposition, instead of a

2-dimensional Fourier transform [13]. In the high finesse limit the plane-wave resonance lineshape is approximated by a Lorentzian factor, and for our normal-incidence Gaussian beam, the lineshape function for the intracavity power becomes

$$L_k(y) = \int_0^\infty \frac{e^{-x}}{1 + (y - kx)^2} dx \quad (2)$$

In equation (2), the dimensionless detuning parameter is $y = 2(\lambda_r - \lambda)/\delta\lambda$ where λ_r is the resonance wavelength at normal incidence and $\delta\lambda$ is the full-width resonance linewidth at half maximum for plane-waves. The other dimensionless parameter k depends on the cavity Q factor $\lambda/\delta\lambda$, the active layer refractive index n , and the beam-waist Gaussian beam radius w , through the relation $k = (\lambda/n\pi w)^2 Q/2$.

Figure 4 displays the dramatic reduction of finesse resulting from even moderate focusing. The calculation has been performed for the case of our sample (cavity Q factor 5000), for various Gaussian beam radii w .

Figure 5 depicts another way of describing qualitatively the origin of this diffraction loss. The oblique plane-wave components tend to escape from the focused beam central region after a few multiple reflections between the mirrors. This limits the effective number of round-trips that participate to the resonance, thus keeping the cavity finesse to a low value. On the contrary, when considering etched microresonators with the geometry of figure 1, total internal reflection along the vertical surfaces keeps the various reflected components within the same region of space. This preserves the original cavity finesse, while the electromagnetic mode has a much reduced volume.

This discussion of course shows the necessity to take fully into account the vertical wave-guiding properties of such microresonators, in particular their transverse mode structure. The problem is complicated by the fact that the 3D geometrical structure of the complete microresonators including the Bragg layer stack regions is fairly complex. However it is

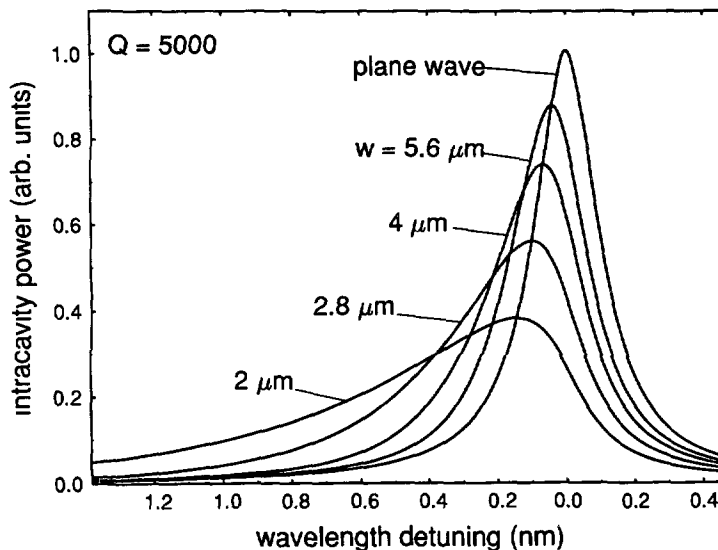


Fig. 4. — Intracavity power resonance function for a plane microcavity of infinite transverse dimensions and various beam radii w .

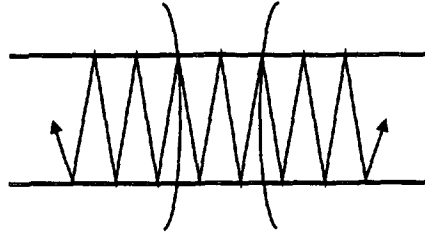


Fig. 5. — Schematic description of the diffraction loss and finesse degradation occurring with tightly focused incident beams.

possible to simplify the problem by treating the refractive index modulation in the Bragg stack regions as a small perturbation of a homogeneous cylindrical waveguide. With this approach, one is led to compute the propagation constants of the various transverse mode a function of optical frequency. From this the periodic boundary conditions imposed by the mirror sections allow to calculate the resonance frequencies of the various transverse modes.

This problem has been studied in more detail in the case of a 6.4 μm diameter microresonator, for which the experimental reflection spectra exhibits a double resonance peak, as shown in figure 6. The spectral separation of the two peaks (0.5 nm) is in good agreement with the values calculated from the effective indices of the fundamental HE_{11} and first higher order TE_{01} , TM_{01} and HE_{21} modes, yielding a splitting of 0.55 nm. For this microresonator size, the nonlinear optical response exhibits a double hysteresis behaviour, as shown in figure 7. This double hysteresis behaviour is somewhat reminiscent of the multistability situation observed in the case where the longitudinal mode spacing is small enough to allow nonlinear switching from one longitudinal mode to the other [17]. In the present case, the longitudinal mode spacing of 84 nm is too large to be responsible for this behaviour. By contrast, the transverse mode splitting shown in figure 6 is of the same order of

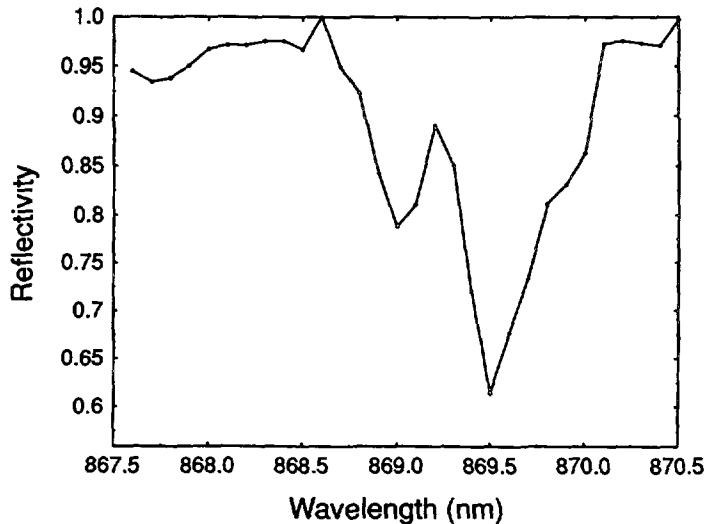


Fig. 6. — Reflection spectra of a 6.4 μm diameter microresonator. The two resonance peaks correspond to the excitation of different transverse modes.

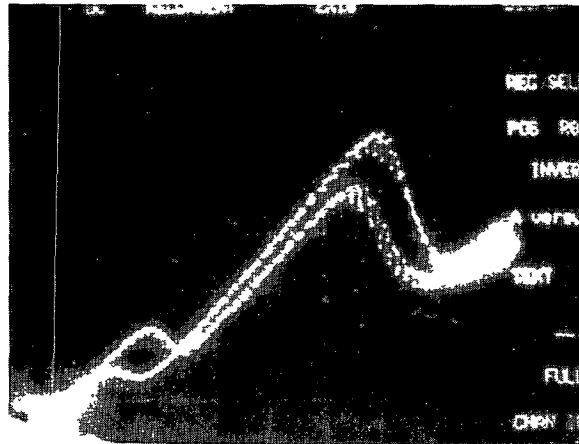


Fig. 7. — Double hysteresis phenomena observed on a $6.4 \mu\text{m}$ diameter microresonator.

magnitude as the typical nonlinear spectral shift observed with GaAs quantum wells [18]. Therefore we interpret this double hysteresis behaviour to the bistable switching between the fundamental and higher order transverse modes.

Such a behaviour was not observed with the $4 \mu\text{m}$ diameter microresonators, even though these waveguides also support multiple transverse modes. However the spectral separation between the fundamental and the first higher-order transverse mode (estimated 1.3 nm) is larger than the 0.4 nm cavity detuning necessary for observing optical bistability. As a result, this multimode character does not prevent us from obtaining a single switching behaviour.

3. Carrier confinement.

The fact that the power density bistability threshold of the $4 \mu\text{m}$ microresonators is approximately the same as that of the unpixelated sample strongly suggests that the carrier lifetime has not been changed significantly by the etching process. This is confirmed by additional studies of the dynamical hysteresis, when the structure is subject to a sinusoidally varying incident intensity at various frequencies in the MHz range. From the scaling law of the dynamical hysteresis thus obtained [19], one can estimate the nonlinear index relaxation time. The relaxation times obtained with this method lead to essentially the same value for the planar sample and the $4 \mu\text{m}$ microresonators.

These observations imply that the vertical surfaces left after the etching step have been subject to some passivation. We have found evidence that the microresonator vertical surfaces are coated by a thin film deposited during the etching process itself. This film is revealed by a selective dry etching of the Si_3N_4 top layer, using a SF_6 RIE, as shown in figure 8. This film, appearing at the top of the microresonators, is semi-transparent to the electron beam used to obtain the micrograph, so its thickness can be estimated to a few hundred nanometers.

The presence of this film can explain several other observations made on this sample. First it explains the smoothness of the vertical surfaces apparent on the SEM micrographs. In addition it chemically stabilizes the vertical surfaces, a point which is of primary concern in the Bragg mirror region where relatively thick AIAs layers could be easily oxydized. After leaving our sample at least six months in a normal laboratory environment, we did not observe a significant degradation, which means that the film also has a role in the chemical passivation of the microresonators. Some Auger characterizations have been performed in order to determine the chemical composition of this film. They indicate the presence of Si, C, N, F, O, Ga, As, Al,

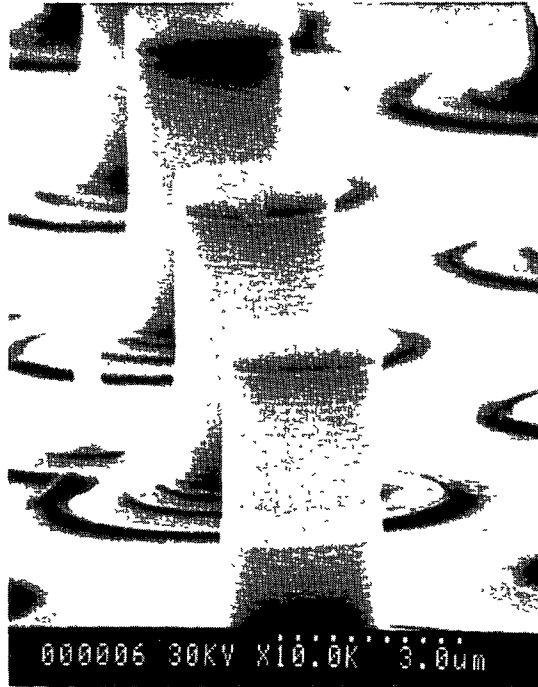


Fig. 8. — Scanning electron micrograph of a microresonator, after removal of the Si_3N_4 top layer by selective dry etching.

with some variation of composition along the lateral surfaces. This chemical complexity comes from the wide variety of chemical species present in the highly reactive plasma. Obviously a more detailed analytic work would be needed in order to fully understand this passivation mechanism.

4. Conclusion.

In conclusion, we have observed for the first time all-optical bistability in GaAs/AlGaAs multiple quantum well microresonators fabricated by reactive ion etching. The bistability threshold power ($70 \mu\text{W}$) was found to be strongly reduced by lateral confinement, i.e. significantly smaller than the minimum value (1 mW) observed on the same sample before etching. The optical confinement allows to achieve a high cavity Q factor in a reduced volume, and leads to the observation of multiple hysteresis loops due to the transverse mode structure of $6.4 \mu\text{m}$ diameter microresonators. Although no surface treatment was realized after the etching process, the low power bistability threshold implies that the surface recombination rate is reasonably small, presumably due to the self-deposition during the etching process of a passivating films.

Acknowledgements.

We gratefully acknowledge the collaboration of A. Izraël, L. Bricard, D. Arquey, C. Mayeux, and C. Dupuis for help in the sample preparation, and of J. F. Bresse for the Auger characterization.

References

- [1] Iga K., Koyama F. and Kinoshita K., Surface Emitting Semiconductor Lasers, *IEEE J. Quantum Electron.* **24** (1988) 1845.
- [2] Jewell J. L., Scherer A., McCall S. L., Lee Y. H., Walker S., Harbison J. P. and Florez L. T., Low-threshold vertical-cavity surface emitting microlasers, *Electron. Lett.* **25** (1989) 1123.
- [3] Venkatesan T., Wilkens B., Lee Y. H., Warren M., Olbright G., Gibbs H. M., Peyghambarian N., Smith J. S. and Yariv A., Fabrication of arrays of GaAs optical bistable devices, *Appl. Phys. Lett.* **48** (1986) 145.
- [4] Jewell J. L., Scherer A., McCall S. L., Gossard A. C. and English J. H., GaAs-AlAs monolithic microresonator arrays, *Appl. Phys. Lett.* **51** (1987) 94.
- [5] Kuszelewicz R., Oudar J. L., Azoulay R., Michel J. C., Brandon J. and Emile O., All-epitaxial GaAs/AlAs nonlinear étalons, *Phys. Status Solidi (b)* **150** (1988) 465.
- [6] Sfez B. G., Rao E. V. K., Nissim Y. I. and Oudar J. L., Operation of nonlinear GaAs/AlGaAs multiple quantum well microresonators fabricated using alloy-mixing techniques, *Appl. Phys. Lett.* **60** (1992) 607.
- [7] De Martini F. and Jacobovitz G. R., Anomalous spontaneous-stimulated-decay phase transition and zero-threshold laser action in a microscopic cavity, *Phys. Rev. Lett.* **60** (1988) 1711.
- [8] Yamamoto Y., Machida S. and Björk G., Microcavity semiconductor laser with enhanced spontaneous emission, *Phys. Rev. A* **44** (1991) 657.
- [9] Yokoyama H., Nishi K., Anan T., Yamada H., Brorson S. D. and Ippen E. P., Enhanced spontaneous emission from GaAs quantum wells in monolithic microcavities, *Appl. Phys. Lett.* **57** (1990) 2814.
- [10] Oudar J. L., Kuszelewicz R., Sfez B., Pellat D. and Azoulay R., Quantum well nonlinear microcavities, *Superlattices Microstructures* **12** (1992) 89.
- [11] Rivera T., Ladan F. R., Izraël A., Azoulay R., Kuszelewicz R. and Oudar J. L., Reduced threshold all-optical bistability in etched quantum well microresonators, *Appl. Phys. Lett.* **64** (1994) 869.
- [12] Azoulay R., Kuszelewicz R., Sfez B., Dugrand L., Oudar J. L., Growth of optical bistable devices by organometallic vapor phase epitaxy, *Ann. Phys. Colloque n 1* (1991).
- [13] Olin U., Model for optical bistability in GaAs/AlGaAs Fabry-Perot étalons including diffraction, carrier diffusion, and heat conduction, *J. Opt. Soc. Am. B* **7** (1990) 35.
- [14] Sfez B. G., Rao E. V. K., Nissim Y. I. and Oudar J. L., Operation of nonlinear GaAs/AlGaAs multiple quantum well microresonators fabricated using alloy-mixing techniques, *Appl. Phys. Lett.* **60** (1992) 607.
- [15] Sfez B. G., Rao E. V. K., Nissim Y., Pellat D. and Oudar J. L., Multiple quantum well microcavities for nonlinear optics, *Nonlinear Opt.* **5** (1993) 171.
- [16] Massa J. S., Buller G. S., Walker A. C., Oudar J. L., Rao E. V. K., Sfez B. G., Kuszelewicz R., Evidence of carrier confinement in nonlinear GaAs/AlGaAs multiple quantum well microresonators fabricated using alloy-mixing techniques, *Appl. Phys. Lett.* **61** (1992) 2205.
- [17] Felber F. S. and Marburger J. H., Theory of nonresonant multistable optical devices, *Appl. Phys. Lett.* **28** (1976) 731.
- [18] Sfez B. G., Oudar J. L., Kuszelewicz R., Michel J. C. and Azoulay R., High contrast multiple quantum well optical bistable device with integrated Bragg reflectors, *Appl. Phys. Lett.* **57** (1990) 324.
- [19] Jung P., Gray G., Roy R. and Mandel P., Scaling law for dynamical hysteresis, *Phys. Rev. Lett.* **65** (1990) 1873.